Supplemental data

Title: Pancreatic ductal adenocarcinoma progression is restrained by stromal matrix

Authors: Honglin Jiang, Robert J. Torphy, Katja Steiger, Henry Hongo, Alexa J. Ritchie, Mark Kriegsmann, David Horst, Sarah E. Umetsu, Nancy M. Joseph, Kimberly McGregor, Michael J. Pishvaian, Edik M. Blais, Brian Lu, Mingyu Li, Michael Hollingsworth, Connor Stashko, Keith Volmar, Jen Jen Yeh, Valerie M. Weaver, Zhen J. Wang, Margaret A. Tempero, Wilko Weichert, Eric A. Collisson

Supplementary material contains the supplemental methods, 3 figures, and 3 tables.

Supplemental Methods

Subjects
All cohorts in this study are summarized in Supplementary Table 3.

1. Rapid autopsy cohort. Primary PDA and metastases were obtained from the Rapid Autopsy Program at the University of Nebraska, as previously described[1]. Tissue microarrays were created from primary and metastatic lesions including lymph nodes, lung, liver, and omentum.
2. Heidelberg cohort. A cohort consisting of 26 patients with primary and/ or metastatic PDA tissue collected at the Department of Medical Oncology, National Center for Tumor Disease (NCT), Heidelberg, Germany[2].
3. Berlin cohort. A cohort investigated previously that received partial pancreatoduodenectomy for PDA between 1991 and 2006 at the Charité University Hospital (Berlin, Germany)[3].
4. Foundation Medicine cohort. Tumor cellularity was examined by next generation sequencing (NGS) in the tumor biopsy samples from patients at UC San Francisco, UC Los Angeles, UC San Diego and UC Davis undergoing Foundation Medicine profiling as a standard of care using the diagnostic terms: pancreas ductal adenocarcinoma and pancreas carcinoma[4].
5. Know Your Tumor cohort. Tumor cellularity was examined by next generation sequencing (NGS) in the tumor biopsy samples from the patients enrolled in the Know Your Tumor Precision Medicine program[5].

Automated stroma quantification. For all cohorts, tissue microarrays were used, and automated stroma quantification was performed as described previously[6]. Briefly, all hematoxylin and eosin (H&E) stained slides were loaded to eSlide Manager and visualized with ImageScope 12.2 (Leica Biosystems, Wetzlar, Germany). Slides were annotated to indicate location and shape of the tumor. Using Definiens Architect XD 2.4 and Tissue Studio 4.1 (both Definiens, Munich, Germany), the annotated images were segmented into different regions of interest (ROIs): tumor epithelium, tumor desmoplasia, and glass. The program then calculated the total area of each ROI. For each specimen, tumor stroma density (TSD) was calculated as follows: TSD = Tumor Desmoplasia Area/Total Tumor Area and averaged over triplicate core for each sample. Two pathologists (K.V. and S.U.) independently reviewed the scanned H&E slides from the Heidelberg cohort and scored primary and metastatic cores as TSD high (≥ 50% of core composed of stroma) or TSD low (<50% of core composed of stroma).

Immunofluorescence staining. Immunofluorescence staining for collagen I (Abcam, clone ab138492) was performed on pancreatic tumors and liver metastases from the rapid autopsy cohort. Percent collagen positive area of total tumor area was digitally quantified and averaged over triplicate cores for each sample.

CT image acquisition and analysis in mice. All CT scans were acquired on a microCT scanner (MILabsVECTor4/CT scanner). An unenhanced CT was first acquired. Following intravenous injection of Omnipaque 350 CT contrast material at a dose of 2ml/kg, images of the whole mouse chest and abdomen were acquired over 10 minutes at a resolution of 100 micron. CT images were analyzed using Osirix MD (Pixmeo, Switzerland). For each mouse, circular region of interest (ROI) were drawn on the tumor and the aorta at the same level on unenhanced and contrast-enhanced images. The CT attenuation values (Hounsfield unit, HU) were recorded. Care was taken to align the two phases of the study when drawing the ROIs. The followings were calculated: Relative tumor enhancement = $(HU_{tumor,\ contrast\text{-}enhanced} - HU_{tumor,\ unenhanced}) / (HU_{aorta,\ contrast\text{-}enhanced} - HU_{aorta,\ unenhanced})$

Mouse studies. All experiments were approved by the Institutional Animal Care & Use Program of the University of California, San Francisco. Derivation of the p53 2.1.1 and FC1245 lines has been described[7, 8]. The cell was first transduced with a lentiviral vector encoding a firefly luciferase. One thousand cells were orthotopically implanted in 6-8-week-old FVB/n or Bl6 mice (Jackson Laboratory) in 20 µL composed of 50% Matrigel. Mice were treated with Ig-G, Gemcitabine (30mg/kg, Sigma) and Anti-LOXL2 mAb AB0023 (30 mg/kg, Gilead, Foster City, CA) intraperitoneally twice a week for 20 days. Tumor growth was monitored by bioluminescent imaging.

Atomic force microscopy. Fresh murine pancreatic tumors were embedded in OCT within a plastic base mold and were snap frozen via direct immersion into liquid nitrogen. Frozen tissue blocks were cut in 25-um sections. Prior to atomic force microscopy (AFM) analysis, each section was thawed, and OCT was washed off by PBS at room temperature. AFM measurements were obtained as described previously[9]. Briefly, AFM measurements were acquired using a MFP3D-BIO inverted optical AFM (Asylum Research) mounted on a Nikon TE200-U fluorescence microscope. Indentation was performed using silicon nitride cantilevers with borosilicate glass spherical tips of 5-um diameter and nominal stiffness 0.06 N/m (Novascan Tech). Cantilevers were calibrated using thermal oscillation. Six 40 um x 40 um AFM force maps were acquired per sample. Tissue stiffness was computed using the Hertz model in Igor Pro (version 6.22A) with a Poisson ratio of 0.5.

Flow cytometry and cell sorting. For sorting of cancer cells and CAFs, single-cell suspensions were prepared and stained with fluorescently conjugated antibodies as following: anti-mouse CD45 (103133; BioLegend), CD326 (EPCAM) (118210; BioLegend), CD31-AlexaFluor 647 (102416; BioLegend), CD140a (PDGFRα) (135907; BioLegend), Ly6C (128015; BioLegend), IL-6 (504503; BioLegend), α-Smooth muscle actin (AC12-0159-05, Abcore). Cells were sorted on the SONY SH800 cell sorter and data were analyzed with FlowJo v10 software.

Statistics. Two-sided two-sample t-tests were used for comparisons of the means of data between two groups. One-way ANOVA was used for comparisons among multiple independent groups. All differences in survival were assessed by Kaplan–Meier analysis and subsequent log-rank test. Associations of markers with each other or clinicopathologic characteristics were investigated by Fisher exact test. Cox proportional hazards model were used to analyze the OS when stratified by high versus low TSD. Two-tailed Mann Whitney U test was used to differentiate the stiffness distribution in AFM measurement.

References

1. Moffitt, R.A., et al., *Virtual microdissection identifies distinct tumor- and stroma-specific subtypes of pancreatic ductal adenocarcinoma.* Nat Genet, 2015. **47**(10): p. 1168-78.
2. Muckenhuber, A., et al., *Pancreatic Ductal Adenocarcinoma Subtyping Using the Biomarkers Hepatocyte Nuclear Factor-1A and Cytokeratin-81 Correlates with Outcome and Treatment Response.* Clin Cancer Res, 2018. **24**(2): p. 351-359.
3. Noll, E.M., et al., *CYP3A5 mediates basal and acquired therapy resistance in different subtypes of pancreatic ductal adenocarcinoma.* Nat Med, 2016. **22**(3): p. 278-87.
4. Frampton, G.M., et al., *Development and validation of a clinical cancer genomic profiling test based on massively parallel DNA sequencing.* Nat Biotechnol, 2013. **31**(11): p. 1023-31.
5. Pishvaian, M.J., et al., *Molecular Profiling of Patients with Pancreatic Cancer: Initial Results from the Know Your Tumor Initiative.* Clin Cancer Res, 2018. **24**(20): p. 5018-5027.
6. Torphy, R.J., et al., *Stromal Content Is Correlated With Tissue Site, Contrast Retention, and Survival in Pancreatic Adenocarcinoma.* JCO Precis Oncol, 2018. **2018**.
7. Collisson, E.A., et al., *Subtypes of pancreatic ductal adenocarcinoma and their differing responses to therapy.* Nat Med, 2011. **17**(4): p. 500-3.
8. Roy, I., et al., *Pancreatic Cancer Cell Migration and Metastasis Is Regulated by Chemokine-Biased Agonism and Bioenergetic Signaling.* Cancer Res, 2015. **75**(17): p. 3529-42.
9. Lopez, J.I., et al., *In situ force mapping of mammary gland transformation.* Integr Biol (Camb), 2011. **3**(9): p. 910-21.

Supplementary Figure 1

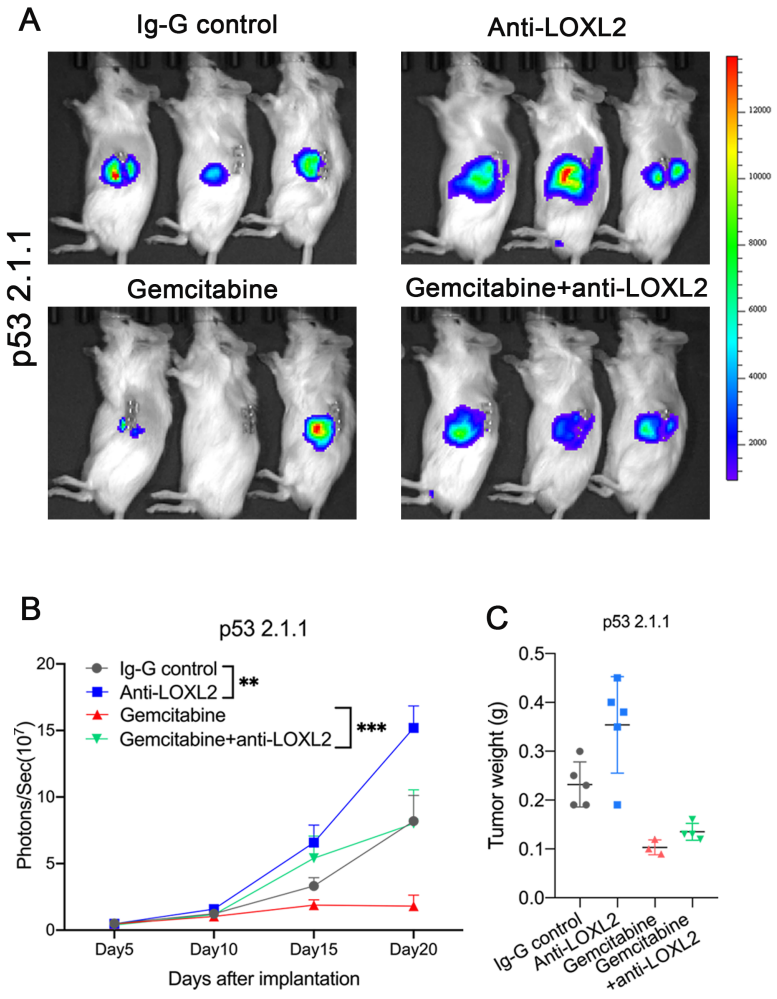

Supplementary Figure 1 Reduction of fibrosis augments murine PDA progression. (**A**) Representative bioluminescent images of p53 2.1.1-fLuc orthotopic pancreas tumor xenografts receiving Ig-G, anti-LOXL2 mAb, GEM and combination of anti-LOXL2 mAb and GEM. (**B**) BLI signal changes (mean ± SEM; error bars) of p53 2.1.1 xenograft, n=5mice/group. Data were analyzed by one-way ANOVA, **p<0.01, ***p<0.001. (**C**) Tumor weight from B was measured at end point.

Supplementary Figure 2

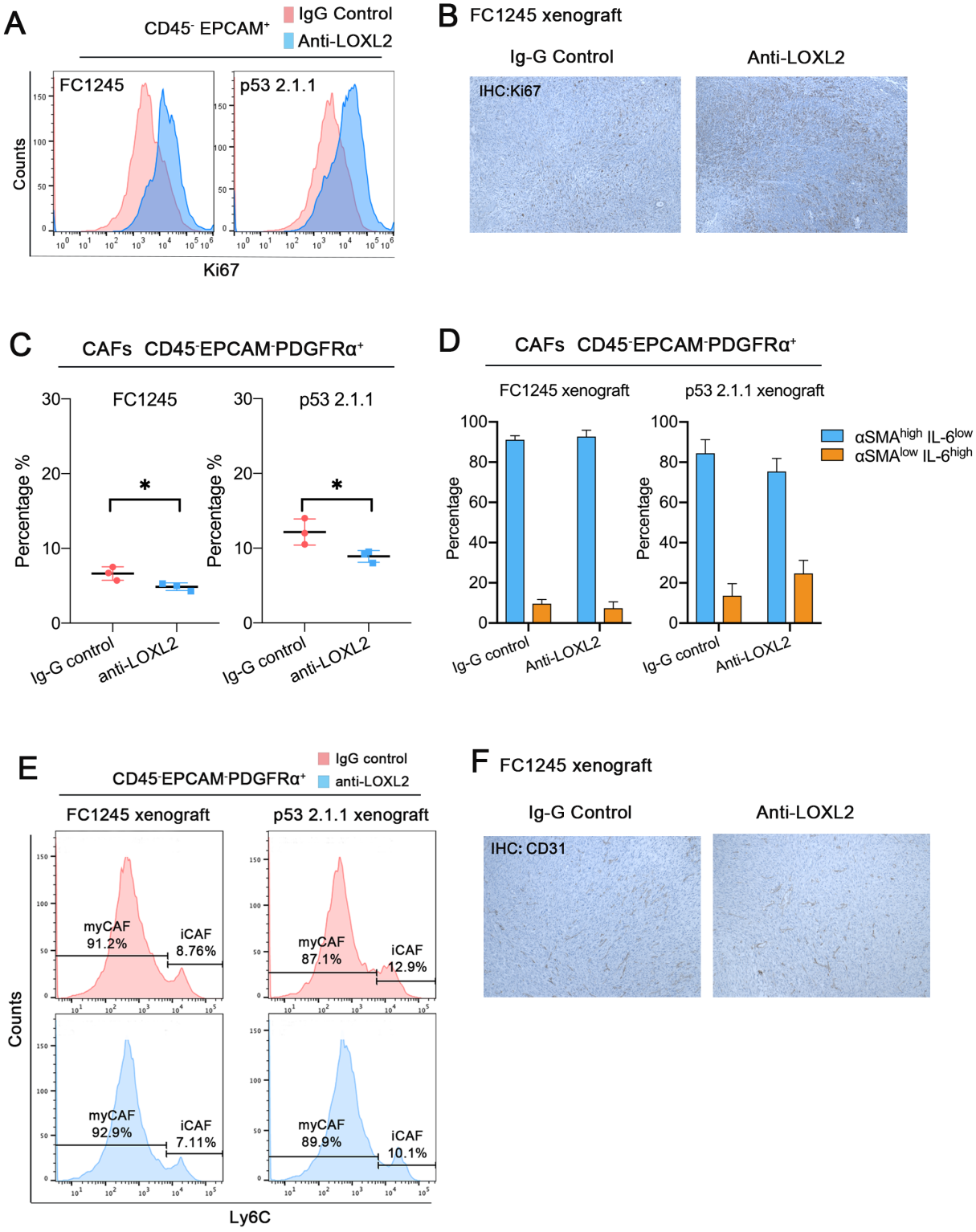

Supplementary Figure 2 The effects of anti-LOXL2 mAb on the tumor microenvironment in PDA. (A) Representative flow cytometric analysis of Ki67 in tumor epithelium cells from FC1245 and p53 2.1.1 orthotopic xenografts upon anti-LOXL2 mAb. (B) IHC of xenografts from FC1245 orthotopic xenografts (10X) stained with Ki67 upon anti-LOXL2 mAb. (C) Flow cytometric analysis of $CD45^{-}EPCAM^{-}PDGFR\alpha^{+}$ fibroblasts in FC1245 and p53 2.1.1 orthotopic xenografts with Ig-G or anti-LOXL2 mAb treatment. Results show mean ± SEM; error bars, n=3mice/group. *P<0.05, unpaired t test. (D) Flow cytometric analysis of αSMA and IL-6 in CAFs from FC1245 and p53 2.1.1 orthotopic xenografts with Ig-G or anti-LOXL2 mAb treatment. Results show mean ± SEM; error bars, n=3mice/group. (E) Representative flow cytometric analysis of Ly6C+ iCAFs and Ly6C- myCAFs in tumors derived from orthotopic transplantation of FC1245 and p53 2.1.1 cells (n=3). The values shown represent the percentages from the parental gate. (F) IHC of xenografts from FC1245 orthotopic xenografts (10X) stained with CD31 upon anti-LOXL2 mAb.

Supplementary Figure 3

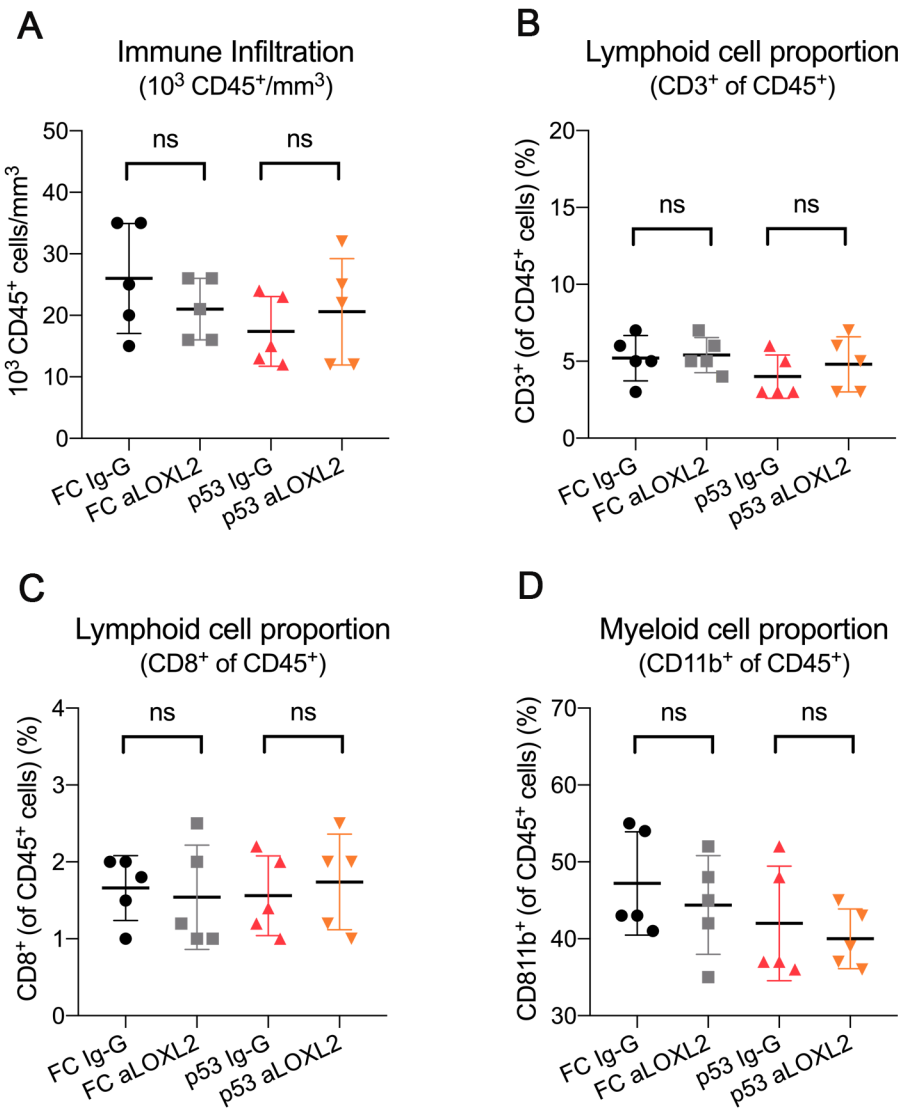

Supplementary Figure 3 Effects of anti-LOXL2 on immune infiltration. (A) Flow cytometric analysis of $CD45^+$ cells normalized to tumor volume in FC1245 and p53 2.1.1 orthotopic xenografts with Ig-G or anti-LOXL2 mAb treatment. Results show mean ± SEM; error bars, n=3mice/group. No statistical difference was found, as calculated by unpaired t test. (B) Flow cytometric analysis of $CD3^+$ pan-T cells in FC1245 and p53 2.1.1 orthotopic xenografts with Ig-G or anti-LOXL2 mAb treatment. Results show mean ± SEM; error bars, n=3mice/group. No statistical difference was found, as calculated by unpaired t test. (C) Flow cytometric analysis of $CD8^+$ T cells in FC1245 and p53 2.1.1 orthotopic xenografts with Ig-G or anti-LOXL2 mAb treatment. Results show mean ± SEM; error bars, n=3mice/group. No statistical difference was found, as calculated by unpaired t test. (D) Flow cytometric analysis of $CD11b^+$ myeloid cells in FC1245 and p53 2.1.1 orthotopic xenografts with Ig-G or anti-LOXL2 mAb treatment. Results show mean ± SEM; error bars, n=3mice/group. No statistical difference was found, as calculated by unpaired t test.

Supplementary Table 1. Patient and disease characteristics stratified by stromal density.

	TSD Low (n=23)	TSD High (n=69)	Total (n=92)	
	n (%)	n (%)	n (%)	p-value*
Age (mean, SD)	64.6 (6.8)	63.4 (10.1)	63.7 (9.3)	0.596
Sex				
Male	13 (56.5)	41 (59.4)	54 (58.7)	0.807
Female	10 (43.5)	28 (40.6)	38 (41.3)	
T Stage				
T1	0 (0.0)	1 (1.5)	1 (1.1)	0.944
T2	6 (26.1)	20 (30.0)	26 (28.3)	
T3	16 (69.6)	43 (63.3)	59 (64.1)	
T4	1 (4.4)	5 (7.3)	6 (6.5)	
N Stage				
N0	6 (26.1)	16 (23.2)	22 (23.9)	0.778
N1	17 (73.9)	53 (76.8)	70 (76.1)	
Overall Stage				
1	3 (13.0)	8 (11.6)	11 (12.0)	0.999
2	18 (78.3)	54 (78.3)	72 (78.3)	
3	1 (4.4)	5 (7.3)	6 (6.5)	
4	1 (4.4)	2 (2.9)	3 (3.3)	
Tumor Grade				
1	0 (0.0)	3 (4.4)	3 (3.3)	0.385
2	10 (43.5)	38 (55.1)	48 (52.2)	
3	13 (56.5)	28 (40.6)	41 (44.6)	
Margins				
R0	13 (65.0)	45 (69.2)	58 (68.2)	0.789
R1	7 (35.0)	29 (30.8)	27 (31.8)	
Pathologic M Stage	22 (95.7)	67 (97.1)	89 (96.7)	0.999
M0	1 (4.4)	2 (2.9)	3 (3.3)	
M1				

*p-values from Fischer's exact test

Supplementary Table 2. Cox proportional hazards model for overall survival.

	HR (95% CI)	p-value
TSD		
TSD High	Ref.	0.022
TSD Low	2.19 (1.11-4.29)	
Sex		
Male	Ref.	0.956
Female	0.98 (0.55-1.770	
T Stage		
T1/T2	Ref.	0.481
T3/T4	1.33 (0.61-2.90)	
N Stage		
N0	Ref.	0.409
N1	1.51 (0.57-4.03)	
Overall Stage		
1	Ref.	
2	0.28 (0.07-1.10)	0.068
3/4	0.92 (0.18-4.72)	0.917
Tumor Grade		
1/2	Ref.	0.917
3	1.50 (0.85-2.64)	
Margins		
R0	Ref.	0.147
R1	1.60 (0.85-3.02)	

Supplementary Table 3. Summary of the all cohorts

Summary of cohorts

Cohort				Analysis
		Primary PDA	Liver metastases	
		Numbers of patients		
Figure 1	Berlin cohort	92	*NA*	Automated Stroma Quantification
Figure 2	Heidelberg cohort	26	26	Automated Stroma Quantification
Figure 2	Rapid autopsy cohort	12	11	IF staining: Type 1 collagen
Figure 2	Foundation Medicine cohort	150	73	Tumor cellularity
Figure 2	Perthera cohort	250	173	Tumor cellularity